energies

MDPI

Review

A Review on Multi-Terminal High Voltage Direct Current Networks for Wind Power Integration

Luís F. Normandia Lourenço [1], Amira Louni [2], Gilney Damm [2], Mariana Netto [3], Monssef Drissi-Habti [2], Samuele Grillo [4], Alfeu J. Sguarezi Filho [1,*] and Lasantha Meegahapola [5]

[1] Center for Engineering, Modeling and Applied Social Sciences, Federal University of ABC, Santo André 09210-580, SP, Brazil
[2] COSYS-IMSE, University Gustave Eiffel, IFSTTAR, F-77447 Marne-la-Vallée, France
[3] COSYS-PICS-L, University Gustave Eiffel, IFSTTAR, F-78000 Versailles, France
[4] Dipartimento di Elettronica, Informazione e Bioingegneria, Politecnico di Milano, Piazza Leonardo da Vinci, 32, I-20133 Milano, Italy
[5] Electrical and Biomedical Engineering, School of Engineering, RMIT University, Melbourne 3001, Australia
* Correspondence: alfeu.sguarezi@ufabc.edu.br

Abstract: With the growing pressure to substitute fossil fuel-based generation, Renewable Energy Sources (RES) have become one of the main solutions from the power sector in the fight against climate change. Offshore wind farms, for example, are an interesting alternative to increase renewable power production, but they represent a challenge when being interconnected to the grid, since new installations are being pushed further off the coast due to noise and visual pollution restrictions. In this context, Multi-Terminal High Voltage Direct Current (MT-HVDC) networks are the most preferred technology for this purpose and for onshore grid reinforcements. They also enable the delivery of power from the shore to offshore Oil and Gas (O&G) production platforms, which can help lower the emissions in the transition away from fossil fuels. In this work, we review relevant aspects of the operation and control of MT-HVDC networks for wind power integration. The review approaches topics such as the main characteristics of MT-HVDC projects under discussion/commissioned around the world, rising challenges in the control and the operation of MT-HVDC networks and the modeling and the control of the Modular Multilevel Converter (MMC) stations. To illustrate the challenges on designing the control system of a MT-HVDC network and to corroborate the technical discussions, a simulation of a three-terminal MT-HVDC network integrating wind power generation and offshore O&G production units to the onshore grid is performed in Matlab's Simscape Electrical toolbox. The results highlight the main differences between two alternatives to design the control system for an MT-HVDC network.

Keywords: multi-terminal HVDC networks; HVDC; modular multilevel converter; control; wind power integration

Citation: Normandia Lourenço, L.F.; Louni, A.; Damm, G.; Netto, M.; Drissi-Habti, M.; Grillo, S.; Sguarezi Filho, A.J.; Meegahapola, L. A Review on Multi-Terminal High Voltage Direct Current Networks for Wind Power Integration. *Energies* **2022**, *15*, 9016. https://doi.org/10.3390/en15239016

Academic Editor: Abu-Siada Ahmed

Received: 19 October 2022
Accepted: 23 November 2022
Published: 29 November 2022

1. Introduction

The participation levels of Renewable Energy Sources (RES) are increasing quickly in power systems around the world and leading to structural changes at an unprecedented pace [1]. RES are variable in nature and they are connected into power systems by static converters which present very different characteristics from traditional synchronous generators that can be dispatched and contribute to system inertia [2,3].

Therefore, the integration of RES has brought new challenges for electrical system operators [1,2]. One of the main challenges is related to the flexibility of power systems, that can be defined as the ability of a power system to adjust power generation and demand in reaction to disturbances [4]. With the decrease in the inertia of the system and the increase in the variability of the operating conditions due to the presence of the RES, a proposal of alternatives to increase the flexibility of systems is necessary [5,6].

The interconnection of neighboring electrical systems presents itself as an interesting alternative from the point of view of flexibility, as it allows the use of resources from the interconnected regions to increase the reliability of the system's operation [7]. Today, the technology for new transmission infrastructure and for reinforcements of existing transmission lines that is best adapted for the future with high penetration levels of RES are the Multi-Terminal High Voltage Direct Current (MT-HVDC) networks [8].

The HVDC technology was firstly deployed in its Current Source Converter (CSC) form [9]. The CSC is a converter based on thyristors and is also known as Line Commutated Converter (LCC). These converters require a connection to a relatively strong AC grid for the commutations, which could not be the case of a converter dominated power system. Moreover, they need to operate with the AC current lagging the AC voltage in a process that requires the availability of reactive power provided by filters [10]. The need for filters considerably increases the size of the converter station which is not a characteristic desired for offshore applications.

With the introduction of the Insulated Gate Bipolar Transistor (IGBT), the Voltage Source Converter (VSC)-based HVDC technology was developed [11]. Since the IGBT is a self-commuting switch, it is possible to fully control the voltage output of the VSC allowing for the independent control of active and reactive power, the connection of passive grids and loads, and reduced converter station size since they do not require a source of reactive power to operate [9,10,12]. For these reasons, VSCs became the preferred type of converter for applications in multi-terminal systems for the integration of offshore wind power [13]. Among the VSC converters, the preferred topology for high voltage applications is the Multilevel Modular Converter (MMC) as it can be applied to high power/high voltage systems. The use of MMCs implies a challenging design of the control system for the converter terminal because of its complex and highly interconnected internal dynamics that include the circulating currents, the energy balance between the phases and the total energy stored in the converter [14].

Therefore, since the stability of the operation of the MT-HVDC network largely depends on the control of its terminals, the design of the control system of each station is crucial for the correct operation of the network [15]. In addition, concerns about the operation of alternating current (AC) systems to which the MT-HVDC network terminals are interconnected require that the design of converter control systems be conducted including the ability to provide support to the AC power grid [16–19]. There is also a challenging task in developing controllers for the operation of the direct current (DC) side of the grid [20].

In this context, the objective of this work is to review relevant aspects regarding the control of MT-HVDC networks for offshore wind power integration. We review the main characteristics of the existing MT-HVDC networks in China and discuss the rising challenges of the control and operation of such networks. The focus of the work is to review the main control strategies for MT-HVDC networks and those of MMC converters, that are essential to achieving the control goals of the network. To illustrate the challenges on designing a control system for an MT-HVDC network, a model for the MMC in the synchronous reference frame is reviewed. Furthermore, a simulation of a three-terminal MT-HVDC network is performed following two of the main DC voltage control strategies to corroborate the technical review of the challenges.

This paper is structured as follows:the concepts of MT-HVDC networks are discussed and the known projects that consider or already adopt this technology are presented in Section 2. Then, in Section 3 we describe the challenges and possibilities of the control of the MMC, the cornerstone equipment for the correct operation of an MT-HVDC network. Section 4 presents a simulation of an MT-HVDC network with three terminals using a $dq0$ frame-based PI controller. Finally, Section 5 presents the conclusions.

2. Multi-Terminal High Voltage Direct Current Networks for Integrating Wind Power and Offshore Resources

At the beginning of the exploration of offshore wind power, the first offshore wind farms were located close to the shore. In these conditions, High Voltage Alternative Current (HVAC) technology was the main alternative for connecting the wind farms to the onshore grid. However, with growing pressure over the noise and visual pollution, offshore wind farms have been pushed further from the shore.

The developments in VSC technology and in submarine power cable design enabled the implementation of efficient high voltage/high power HVDC transmission systems that became the favored technology for integrating offshore wind power [13]. Moreover, given the improved controllability of VSCs over CSCs, it became possible to operate in a multi-terminal framework, enabling to envision super transmission grids for integrating offshore wind power and neighbor power systems.

An MT-HVDC grid interconnecting a cluster of offshore wind farms and oil & gas (O&G) production platforms is shown in Figure 1. The main advantages on adopting this concept is the lack of reactive power within the transmission system (with the associated voltage stability issues), lowering power losses, and the possibility to integrate asynchronous grids.

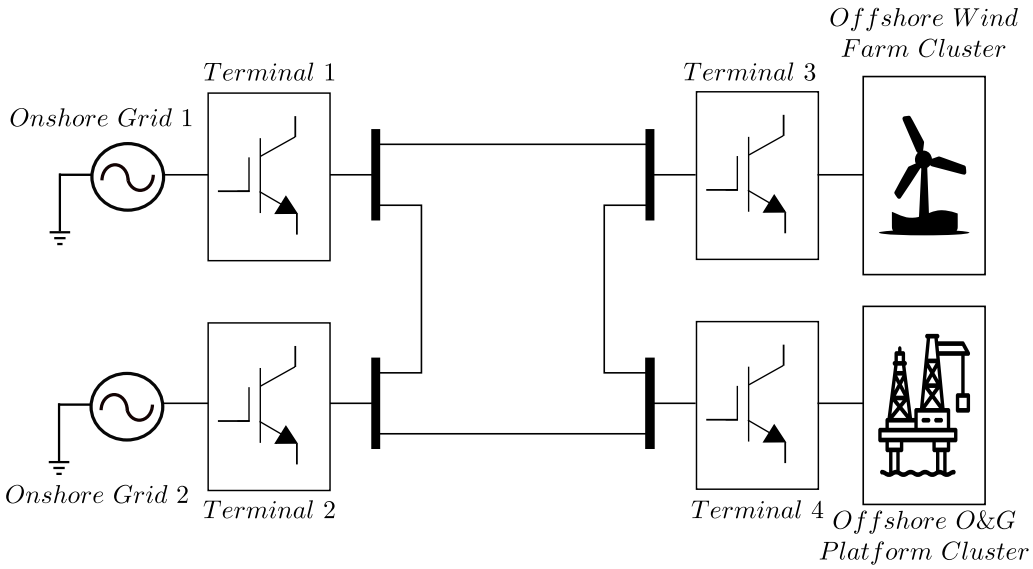

Figure 1. A Multi-Terminal HVDC network for integrating offshore wind power and offshore O&G production units to the onshore grid in two connection points.

In Europe, MT-HVDC networks are envisioned as the basis for the future European Supergrid [21,22] since the early 2000s. To achieve ambitious sustainable goals regarding electric power production, Europe aims to integrate high amounts of offshore wind power in the North Sea to England, France, Germany and Norway. Moreover, offshore O&G production units could receive electric power from the shore, lowering the emissions in their production, as O&G are still expected to play a major role in the energy transition [23–25]. In the South, the European grid could be interconnected to Northern Africa to integrate the production of high levels of solar power.

In China, the world's first MT-HVDC network based on the VSC-HVDC technology was built in 2013 [26]. The grid was conceived as a three-terminal pilot project with transmission capacity of 200 MW at $\pm$160 kV to interconnect the wind farms from Nanao island into the onshore grid. It is also foreseen that this grid can be expanded to four terminals if the power capacity generation of wind power increases. Nowadays there are two more MT-HVDC grids operating in China.

The Zhoushan archipelago in China is a region rich in wind energy production, but it lacked grid reliability and flexibility. In 2014, a five terminal MT-HVDC grid was

commissioned to solve reliability problems and to improve the stability of the system. The terminals of the system were constructed at 400 MW, 300 MW and three of them at 100 MW installed capacity at ±200 kV [27]. Moreover, it allowed the system to operate with higher levels of wind power with improved flexibility.

Finally, commissioned in 2019, the Zhangbei MT-HVDC grid was conceived to enable the supply of 3000 MW of wind power to Beijing for the Winter Olympics held in the beginning of 2022 [28]. The multi terminal grid is comprised of four terminals, two of which are the collecting terminals of wind farms and one is a pumped hydro storage facility that enables balancing the power face to load and wind variations [29]. With recent advancements in MMC-based VSC-HVDC transmission systems, the HVDC technology for this grid reached the power level of 3000 MW at ±500 kV found at two of four of the terminals of the Zhangbei grid [30]. The remaining two terminals are rated 1500 MW at ±500 kV. The operating MT-HVDC grids in China are summarized in Table 1.

Table 1. Operational MT-HVDC networks in China with VSC technology

Project	Power Capacity	Voltage	Operational	Ref.
Nanao Island	3 × 200 MW	±160 kV	2013	[26]
Zhoushan Archipelago	400 MW, 300 MW, 3 × 100 MW	±200 kV	2014	[27]
Zhangbei	2 × 3000 MW, 2 × 1500 MW	±500 kV	2019	[28–30]

There are still a wide number of challenging open problems regarding MT-HVDC networks for wind power integration as seen in Figure 2. The installed capacity of each terminal of an MT-HVDC network can be big enough to exert influence on the dynamics of the surrounding power system. Hence, control techniques need to be developed to enable a suitable dynamic behavior from the terminals of the MT-HVDC network. Additionally, power engineers have a wide experience in the control and operation of HVAC power systems accumulated in more than 100 years [31,32]. The existence of real MT-HVDC grids is quite recent and unanticipated problems may appear in the upcoming years that will demand new solutions.

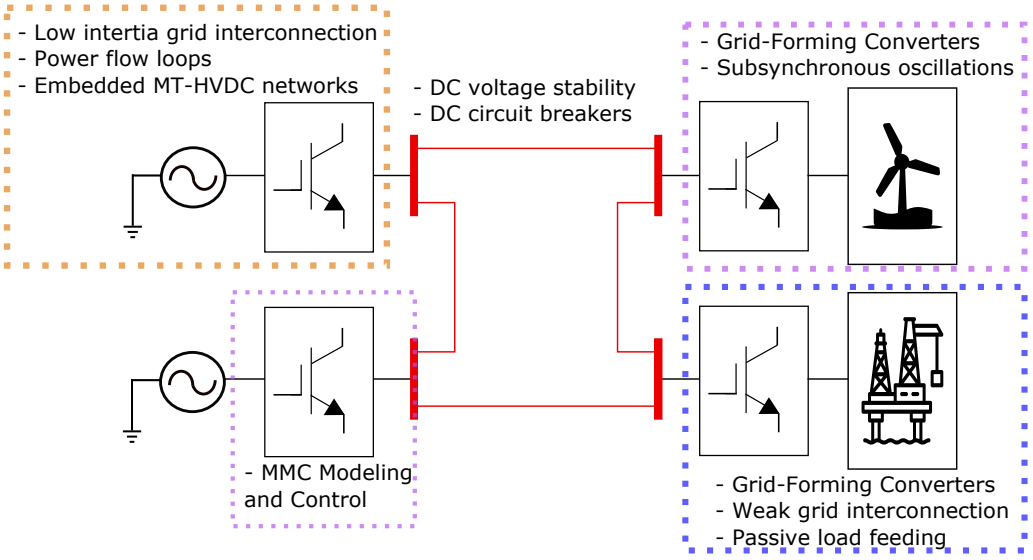

Figure 2. Open problems and challenges in the control and operation of MT-HVDC networks.

A subset of the rising control problems is related to the integration of MT-HVDC networks to the existing power system. They are suitable candidates for a new power transmission infrastructure as reinforcements of existing power systems, leading the way to embedded HVDC links in a mixed AC/DC power system [8,33,34]. A rising phenomenon

that needs to be addressed in this context is the existence of power loops within the power system [35,36]. The interaction between the wind farms and the converter stations is also prone to problems such as the sub-synchronous oscillations [37]. Furthermore, with the power system transition leading into low inertia power systems and the decrease in the number of fossil fuel-based synchronous generators, converter-based resources such as the terminals of MT-HVDC networks might act as Grid-Forming Converters [38–40]. The control problem of an MMC acting as a Grid-Forming Converter is a challenging task that is currently under investigation by the scientific community (see [41–44]).

Regarding stability, works such as [33,34] focused on proposing control strategies to ensure the stability of embedded HVDC links that were extended to embedded MT-HVDC networks in [8]. The DC voltage stability of an MT-HVDC network is also a critical aspect that needs to be investigated. In [45], the damping torque concept is expanded from AC systems for analyzing the DC voltage stability of an MT-HVDC network in the context of wind power integration. In [46], a small signal model is used to investigate the origins of DC voltage oscillations in MT-HVDC networks and also evaluates the impact of the control imposed dynamics of the converters on the oscillations. Further work by [47] investigates the impacts of parameter mismatch between converter stations of an MT-HVDC network on the critical CD voltage stability.

Another rising challenge is the protection of the MT-HVDC grid, as the DC current does not cross the zero value as does the AC current [48]. Different techniques have been proposed as an alternative for the protection of MT-HVDC networks such as the Z-source DC breaker [49] and the hybrid DC circuit breaker [50]. Additionally, the impacts of DC breakers in the stability of the DC voltage is a concern investigated by [51] that should be under the spotlight in upcoming years as new developments on DC circuit breaker technology becomes available.

In this work, we focus the review effort on the control of MT-HVDC networks and on the control of the MMC converter stations. In the following section, a model of the MMC is presented to illustrate the challenges on designing a control system to such a nonlinear and highly interconnected plant. We also discuss the main techniques for the control of the DC voltage and for integrating the converter stations to the grid.

3. Control of the MT-HVDC Network

In this section, the main challenges associated with the control of MT-HVDC networks are discussed. First, the operation of the MT-HVDC network is introduced alongside with its control objectives. Then, the rising challenges are introduced and briefly discussed. As the main equipment to be controlled is the MMC converter, special attention is given to the modeling and control of this converter in active and reactive power control (PQ-control) and DC voltage control operation modes.

3.1. Control of the MT-HVDC Network

The operation of an MT-HVDC network is a complex task. The main objective is to maintain the DC voltage stable whilst achieving the control targets at each terminal of the network. In this scenario, the variations in the DC voltage reflect the power imbalance between power generation and consumption on the MT-HVDC network, just as frequency variations indicate power mismatches in AC systems. Hence, the DC voltage must be kept within a threshold to ensure the reliable operation of the converters and consequently of the MT-HVDC network. For instance, Ref. [52] suggests a threshold of $\pm 10\%$ of the rated DC voltage value and Ref. [53] suggests that the DC voltage must be within $\pm 5\%$ of its rated value. These values are established taking into account variables such as the security constraints on the modulation index of the converters and the insulation levels of he switching elements [53].

In fact, early publications on MT-HVDC networks were focused on achieving a stable DC voltage control. In traditional MT-HVDC control strategies, one of the network's terminals is chosen as the reference for the control of the DC voltage (slack bus) while

the remaining terminals are focused on PQ controllers. This operation strategy is known as master/slave operation [12]. The master converter is the one responsible for the DC voltage control; the slaves are the converter stations responsible for the control of the active and reactive power flowing to/from the MT-HVDC grid. A downside of the master/slave control strategy is that all the burden of the DC voltage control is placed upon a single converter of the MT-HVDC network.

Therefore, to share the burden of the control and improve DC voltage stability, droop control strategies were proposed [12,54]. To improve the DC voltage stability, the active power references sent to the terminals are modulated by a DC voltage droop control strategy [54,55]. The modulation consists on modifying the active power reference proportionally to the DC voltage deviation to achieve the power balance of the network within a new power balance [56]. The references might be later updated by a secondary DC voltage controller that re-dispatches the active power reference values to each terminal to eliminate the steady-state error on the DC voltage. More complex networks might call for a higher degree of sophistication of the DC voltage droop control such as the coordinated action proposed by [57] or the adaptive droop proposed by [58].

In a movement to improve the stability of the DC voltage by having more than one terminal sharing the control of the DC voltage, the authors in [59] proposed a distributed DC voltage control. Their paper was focused on the integration of offshore wind farms and an optimal power flow was proposed for obtaining the DC voltage references for multiple terminals controlling the DC voltage. With this method, the risk of power oscillations due to multiple terminals acting in the control of DC voltage is reduced.

With the increasing penetration of converter interfaced resources, the power system is undergoing a major change in its structures. The overall inertia levels of the power system decreases as converter penetration increases, therefore, there is a concern over frequency stability that must be addressed by new control strategies for converters. For instance, in [60] a frequency droop component was added to the DC droop control of the MT-HVDC network to provide frequency support to the AC side. In [61], an adaptive droop control strategy was proposed where a $V - I - f$ characteristic is derived to adjust the DC voltage reference value to provide frequency support to the nearby AC system. Adaptive adjustments of the droop coefficients to improve the support from undisturbed networks is proposed in [62] to diminish the disturbances in the DC network to avoid a secondary event after the first frequency disturbance is cleared. Aiming to contribute with the reduction/elimination of a secondary frequency disturbance arising from the recovery of the rotor speed from offshore wind farms, adaptive droop control strategies were also proposed in [63,64].

To increase the flexibility of the operation of the overall system, including the MT-HVDC grid and all of the interconnected AC power systems, [65] proposes a coordinated control strategy that allows for mutual frequency support between the AC grids interconnected by the MT-HVDC network. As a result, power reserves can be allocated considering the most efficient resources of each AC network. In [8], a new control strategy is proposed motivated by concerns over the stability of the system. Through active power modulations, the authors develop a distributed control structure for an MT-HVDC network that is capable of improving rotor angle stability and transient stability.

The above control strategies for MT-HVDC networks are enabled by modulation of the active power reference value. Hence, they all rely on the inner control level corresponding to the control of the power converters at each terminal. In the following subsections, we present the model and the main strategies for controlling the terminals of the MT-HVDC network according to their role in the system as a master/slave terminal or as droop-controlled terminal to share the DC voltage control burden.

3.2. The MMC Converter in MT-HVDC Networks

Both the master and the slave converter station control problems are directly linked to the control of the power converter associated with each terminal. In the context of modern

converter stations for high power/high voltage applications, the preferred topology for the MT-HVDC network's terminals is the MMC, whose average electric model is shown in Figure 3.

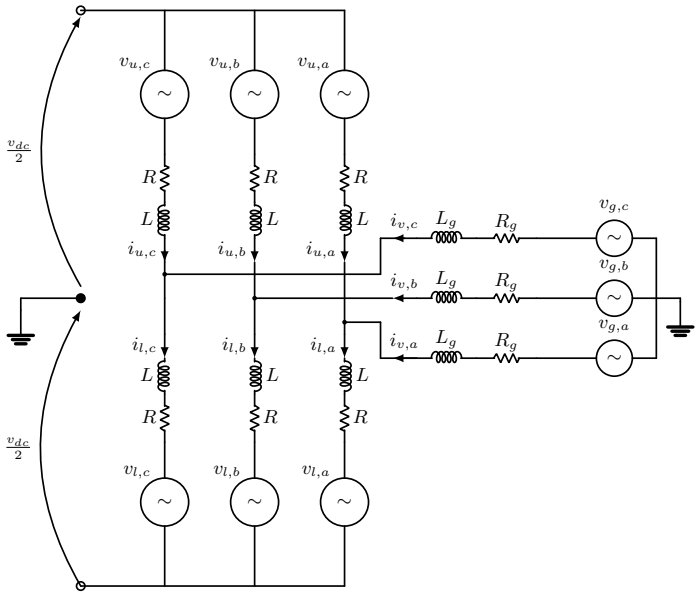

Figure 3. Arm Average Model (AAM) of an MMC-HVDC station connected to the electric grid in Grid Following Mode.

The control problem associated with an MMC converter is to generate a three-phase voltage at the converter output that meets the exchanged active and reactive power targets with the electric grid. In an MMC, the voltage generation at the converter output is carried with additional degrees of freedom when compared to the traditional 2-level VSC by manipulating the six voltages $v_{a,b,c}^{u,l}$ of each converter arm, which are the voltages synthesized by the upper and lower arms, respectively denoted by the superscripts u and l from phases a, b and c. The voltage of each arm is generated by connecting a certain number of submodules as defined by the system control. Since a submodule can be turned on and off independently from one another, there is no guarantee that the submodules will charge and discharge uniformly.

The consequence of the uneven changes in the voltage of the submodules is a temporary voltage unbalance between the converter's arms and legs that results in currents circulating inside the converter. These circulating currents can transport energy across the converter resulting in mismatches between the total voltage of each leg and also in the balance between the energy stored in upper and lower arms of a phase [66]. Therefore, the control problem associated with the MMC has increased complexity compared to 2-level VSC. In addition to meeting the active and reactive power exchanges with the grid, it is necessary to control the internal converter dynamics (circulating currents, energy balance and stored energy) to ensure its stable operation.

The control strategies proposed for the MMC aim at determining the number of submodules that should be turned on at each interval so that the desired voltage is obtained at the converter output. This number can be determined directly [66] or indirectly by a modulation index [67]. The control strategies already proposed in the technical literature can be classified into non-energy controlled and energy controlled approaches.

The non-energy controlled approaches do not have a dedicated control loop for the converter stored energy such the open-loop strategy [68], the direct voltage modulation [69] and the circulating current suppression control [70]. These methods consist on obtaining the insertion index, i.e., the number of submodules that should be turned on for each converter arm, using estimates of the total DC voltage. Although the non-energy controlled

approaches are asymptotically stable [71,72], the convergence speed of the converter energy dynamics is determined by the values of the circuit components.

On the other hand, the energy controlled approach employs control loops for the converter energy dynamics [66,67,73]. Therefore, it is possible to determine the convergence speed of the internal energy by tuning the controllers.

In the following subsection, the modeling and possible solutions to the energy controlled problem of the MMC for both master and slave terminals of an MT-HVDC network are presented.

3.3. Modeling and Control of a PQ-Controlled Terminal

As mentioned, the adoption of the MMC increases the complexity in the modeling and control of the MT-HVDC network. Therefore, several works dedicated to the modeling of the MMC have been proposed. Models in the *abc* frame were developed by [66,67,69,74], in the $\alpha\beta 0$ frame by [16,17,73] and in the $dq0$ frame by [75–77]. To showcase a controller design, this paper considers the bilinear model developed by [75] in the $dq0$ frame.

By defining the output converter currents in the d and q references $i_{v,dq}$ as:

$$i_{v,j} = -i_{u,j} + i_{l,j} \tag{1}$$

where $i_{u,j}$ is the upper arm current and $i_{l,j}$ is the lower arm current of the component j, $j = d, q$.

The circulating currents $i_{circ,dq0}$ are defined as:

$$i_{circ,k} = \frac{i_{u,k} + i_{l,k}}{2} \tag{2}$$

where $k = d, q, 0$.

Furthermore, defining the following auxiliary input variables [16] as:

$$e_{v,dq} = v_{u,dq} - v_{l,dq}, \qquad e_{sum,dq0} = \frac{v_{u,dq0} + v_{l,dq0}}{2} \tag{3}$$

The following MMC model given by (4)–(10) can be obtained:

$$\dot{i}_{v,d} = -\frac{R_{eq}}{L_{eq}} i_{v,d} + \omega i_{v,q} + \frac{1}{L_{eq}} e_{v,d} + \frac{2}{L_{eq}} v_{g,d} \tag{4}$$

$$\dot{i}_{v,q} = -\omega i_{v,d} - \frac{R_{eq}}{L_{eq}} i_{v,q} + \frac{1}{L_{eq}} e_{v,q} + \frac{2}{L_{eq}} v_{g,q} \tag{5}$$

$$\dot{i}_{circ,d} = -\frac{R}{L} i_{circ,d} + \omega i_{circ,q} - \frac{1}{L} e_{sum,d} \tag{6}$$

$$\dot{i}_{circ,q} = -\omega i_{circ,d} - \frac{R}{L} i_{circ,q} - \frac{1}{L} e_{sum,q} \tag{7}$$

$$\dot{i}_{circ,0} = -\frac{R}{L} i_{circ,0} - \frac{1}{L} e_{sum,0} + \frac{1}{L} v_{dc} \tag{8}$$

$$\dot{W}_v = \frac{3}{4} e_{sum,d} i_{v,d} + \frac{3}{4} e_{sum,q} i_{v,q} - 3 e_{v,d} i_{circ,d} - 3 e_{v,q} i_{circ,q} \tag{9}$$

$$\dot{W}_h = -\frac{3}{2} e_{v,d} i_{v,d} - \frac{3}{2} e_{v,q} i_{v,q} + \frac{3}{2} e_{sum,d} i_{circ,d} + \frac{3}{2} e_{sum,q} i_{circ,q} + 3 e_{sum,0} i_{circ,0} \tag{10}$$

where R and L are the arm resistance and inductance, respectively, and R_{eq} and L_{eq} are defined by:

$$R_{eq} = R + 2R_g, \qquad L_{eq} = L + 2L_g \tag{11}$$

The converter energy W_h is obtained by adding the energy stored in the upper and lower arms and the energy difference W_v is obtained by subtracting them as:

$$W_h = W_u + W_l, \qquad W_v = W_u - W_l \tag{12}$$

and the energy stored in the upper arms W_u and in the lower arms W_l are given by:

$$W_u = \sum_{j=a,b,c} \sum_{i=1}^{m} C_{SM} V_{u,j,i}^2, \qquad W_l = \sum_{j=a,b,c} \sum_{i=1}^{m} C_{SM} V_{l,j,i}^2 \tag{13}$$

where C_{sm} is the capacitance of the submodules.

The structure used to control the active and reactive power exchanges with the electric grid is similar to the one used for the 2-level VSC. A current controller can be implemented in the dq synchronous reference frame when the converter is connected to a balanced system, which is generally the case for the transmission level. Then, the current controller is responsible for generating the auxiliary inputs $e_{v,dq}$ that are used to control the output currents $i_{v,dq}$ to their respective reference values $i_{v,dq,e}$ given by:

$$i_{v,d,e} = \frac{2\overline{P}}{3v_{g,d}}, \qquad i_{v,q,e} = -\frac{2\overline{Q}}{3v_{g,d}} \tag{14}$$

If a droop control strategy is implemented for the DC voltage, the reference $\overline{P}$ is obtained as follows:

$$\overline{P} = P^* + K_d(v_{dc} - \overline{v}_{dc}) \tag{15}$$

where P^* is the active power reference provided by the system operator, K_d is the DC voltage droop coefficient, v_{dc} is the measured DC voltage and $\overline{v}_{dc}$ is the DC voltage reference value.

To establish an energy controlled strategy, a circulating current controller is needed and should be responsible for tracking the circulating current references by generating the auxiliary inputs $e_{sum,dq0}$. The references $i_{circ,dq0,e}$ are determined by an upper-level controller comprised by the energy controller and the energy difference controller. The first is responsible for tracking the total energy stored in the converter by manipulating the reference trajectory $i_{circ,0,e}$, whilst the latter is responsible for keeping the energy balance by manipulating the reference trajectory $i_{circ,d,e}$ as discussed in [78].

From the auxiliary inputs $e_{v,dq}$ and $e_{sum,dq0}$, the Arm Voltage Calculation block is able to obtain the six arm voltages $v_{abc}^{u,l}$ in the abc frame. Then, a modulation scheme is used to determine the number of submodules that need to be turned on to generate the desired voltage at each arm. This information is finally sent to a sorting algorithm that is responsible for choosing which of the submodules must be turned on. When the current is charging the submodule capacitor, it selects the submodules with the lowest voltage and when the current is discharging the SM capacitor, the algorithm selects the submodules with the highest voltage [79–81].

3.4. Modeling and Control of a DC Voltage-Controlled Terminal

Differently from 2-level VSC converter stations, MMC converter stations do not have a large capacitor bank on their interface with the DC link. Instead, they have smaller capacitances distributed across the converter submodules, turning the DC voltage control in a challenging task [82]. So far, research papers can be found in a much greater number dedicated to the control of active and reactive power exchanges for MMC converters while the DC voltage problem is often overlooked, except by a few handful of works.

In [83], a multivariable control strategy relying on four PI controllers is proposed for controlling the DC voltage of HVDC systems. In [17], the effect of the cable capacitance in the DC voltage control of an HVDC link based on MMCs is investigated, analyzing three different controller structures: classic control, crossed control (when $i_{circ,0}$ is used to control v_{dc}) and weighted control. The weighted control uses a linear combination of

classic and crossed controls to generate its input signal. In [84], a control strategy using the classic v_{dc} structure from 2L-VSC is applied, but the energy control is modified to reflect the changes of the DC voltage in the converter energy. In [85], a virtual capacitor method is proposed for controlling the DC voltage in point-to-point HVDC transmission systems. This technique consists of adding a virtual capacitor in parallel with the cable capacitance to represent the energy stored in the MMC.

However, despite the challenges in the control of the DC voltage when an MMC converter is considered, the modeling is quite similar to the one presented in the previous section. One equation must be added to include the dynamics of the DC voltage at the terminal as follows:

$$\dot{v}_{dc} = \frac{i_S}{C} - \frac{3}{2Cv_{dc}}\left(e_{v,d}i_{v,d} + e_{v,q}i_{v,q}\right) \tag{16}$$

then, the complete model is given by (4)–(10) and (16).

For the master converter station, the reference for the $i_{v,d}$ is given by a DC voltage controller. Generally, the DC voltage controller generates a reference $i_{v,d,e}$ such that the power balance in the DC link is met, thus regulating the DC voltage [86–88].

A different overall structure for the controller of the master terminal could be adopted as proposed in [17]. The circulating current reference $i_{circ,0,e}$ could be used instead of the $i_{v,d,e}$ current component reference to control the DC voltage in the MT-HVDC network. Then, the output current reference $i_{v,d,e}$ is used to control the energy stored in the converter. Therefore, this control structure was described by [17] as a crossed control structure.

4. Simulations of an MT-HVDC Network for the Integration of Wind Power

To illustrate the challenges on the control of MT-HVDC networks for integrating offshore wind power and other offshore power systems, simulations of two control methods are shown. The MT-HVDC network with three terminals shown in Figure 4 is considered for the simulations.

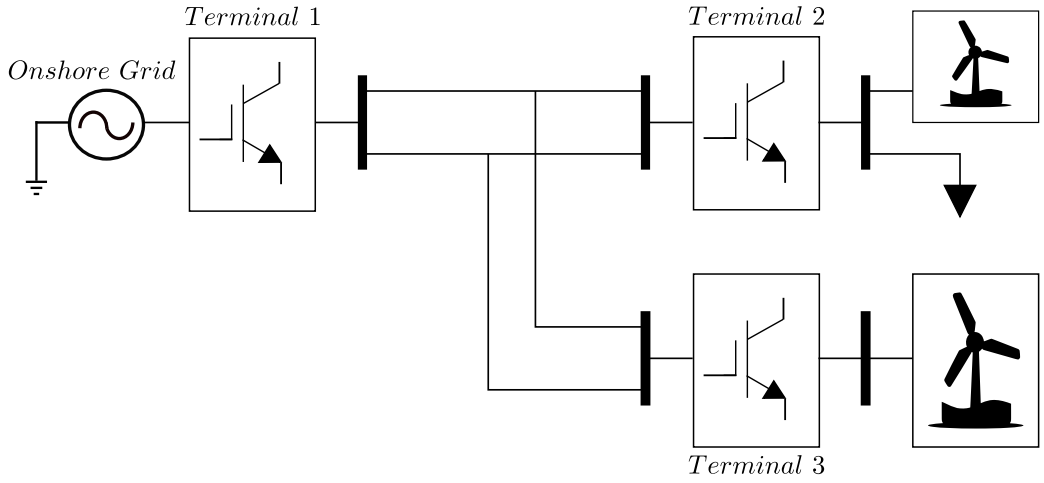

Figure 4. Three-terminal MT-HVDC network simulated in Matlab's Simscape Electrical.

Terminal 2 is considered as the point of connection of a cluster of offshore wind farms and a cluster of O&G platforms represented by the load. Terminal 3 connects a cluster of offshore wind farms to the MT-HVDC network. Terminal 1 is considered as the connection of the MT-HVDC network for integrating offshore wind power to the onshore grid. In the following subsections, the possible control systems considering the master/slave and the droop control strategy are detailed.

4.1. Control Systems for MT-HVDC Networks Based on the dq Frame

In this subsection, we present a possible implementation of a PI-based controller for the MMCs in an MT-HVDC network in master/slave and droop control strategies. A main

assumption is that the systems that the terminals are connected to are balanced. Therefore, the 0 component of the output current i_v can be neglected. The cascaded structure of the controller presented in this section is based on the controllers developed by [67] in the *abc* frame and by [17] in the $\alpha\beta$ frame.

4.1.1. Control of the Slave Terminals

The slave terminals are controlled in PQ-mode. Therefore, the objective is to regulate the active and reactive power of the converter to the prescribed set-point values given by the system operator.

Thanks to the independent active and reactive power control in VSC converters, the PQ control can be reduced by a current control by using (14) to calculate the current references. Then, the output current components can be regulated using a PI controller as seen in Figure 5:

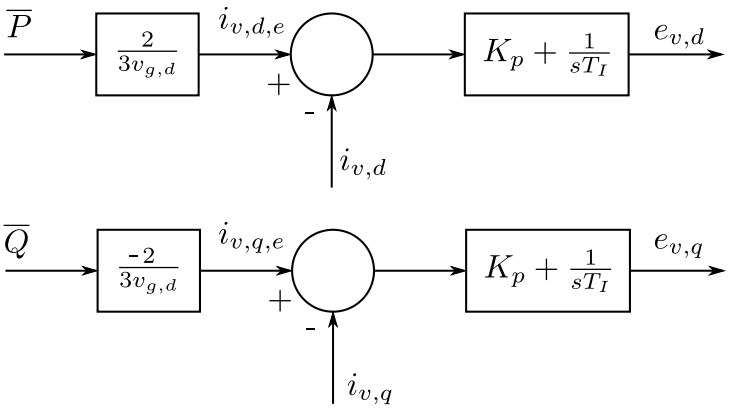

Figure 5. Slave terminal output current controller.

where $\overline{P}$ is the active power reference value, $\overline{Q}$ is the reactive power reference value, K_p is the proportional gain and T_I is the integral time of each PI controller.

The auxiliary control inputs $e_{v,d}$ and $e_{v,q}$ generated by the output current controller are sent to the arm voltage calculation and modulation for processing. There, they are combined with the auxiliary control inputs $e_{sum,d}$, $e_{sum,q}$ and $e_{sum,0}$ generated by the internal dynamics controller described bellow to obtain the arm voltages $v^{u,l}_{a,b,c}$ before they are processed by the modulation to generate the gating signals.

For regulating the internal dynamics of the MMC converter, the control scheme shown in Figure 6 is adopted, where $\overline{W}_v$ is the reference value for the energy difference, $\overline{W}_h$ is the reference value for the converter stored energy, K_p is the proportional gain and T_I is the integral time of each PI controller.

As mentioned in the previous section, the reference value $i_{circ,d,e}$ is used to regulate the energy difference W_v. The value $i_{circ,d,e}$ is generated by a PI controller that has the energy difference error as input. Then, an inner circulating current loop is used to regulate $i_{circ,d}$ to the specified value given by the upper level controller.

For the converter energy, a similar structure is used. The reference value $i_{circ,0,e}$ is used to regulate through a PI controller the energy stored in the converter. An inner circulating current control loop is used to regulate $i_{circ,0}$ to the reference value provided by the upper level controller.

Finally, the $i_{circ,q}$ component is regulated to the reference value $i_{circ,q,e} = 0.$ to lower power losses as in [70,78].

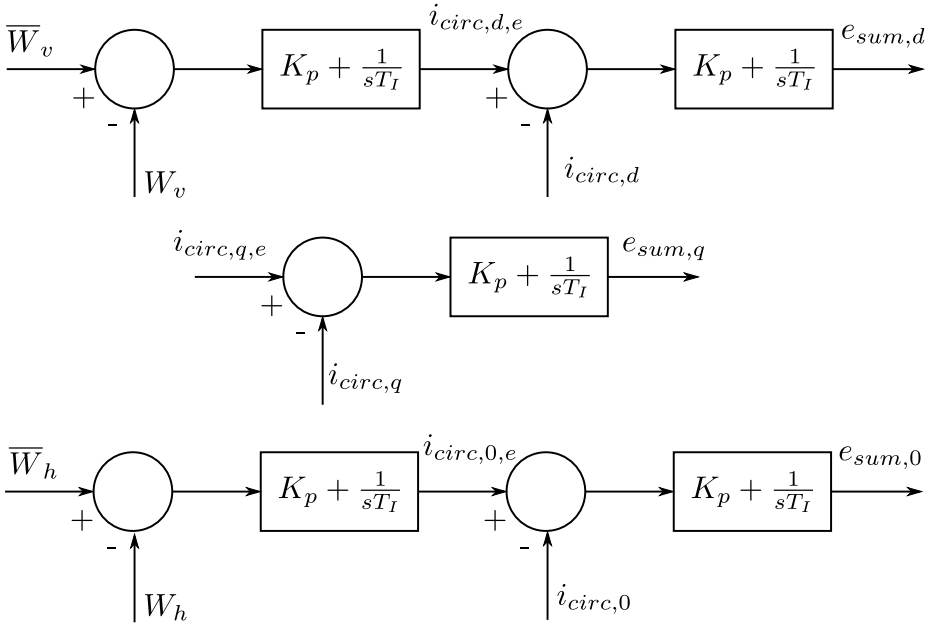

Figure 6. Slave terminal internal dynamics cascaded control structure.

4.1.2. Control of the Master Terminal

The master terminal is the one responsible for the DC voltage control. Thanks to the independence of active and reactive power control inherent to VSCs, the $i_{v,d}$ component in the slave terminal, associated with the active power, can now be used to regulate the DC voltage. In addition, in the master terminal, it is desirable to control the reactive power Q through the current component $i_{v,q}$.

The cascaded control structure for the master terminal is shown in Figure 7, where $\overline{v}_{dc}$ is the reference value for the DC voltage.

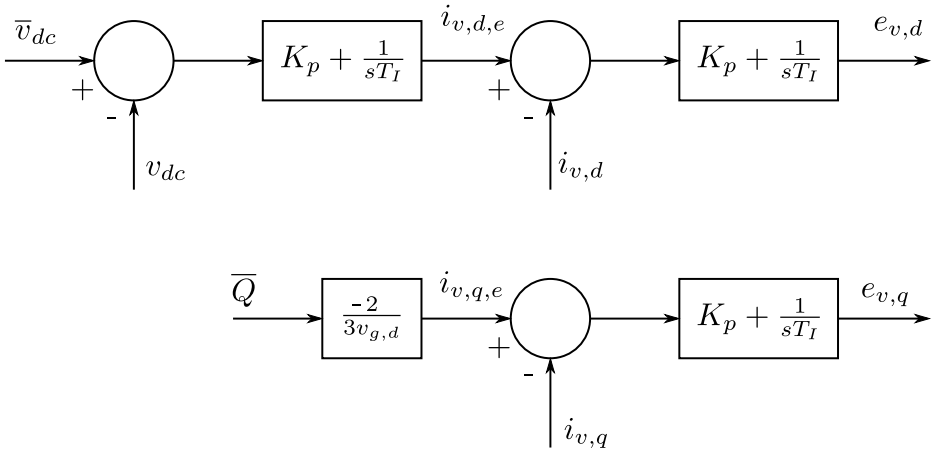

Figure 7. Master terminal cascaded control structure for regulating the DC voltage and the output currents.

For the simulations presented in this work, the same controller for the internal dynamics from the previous subsection is adopted. It is worth mentioning that, as seen in the literature [85,89], the DC voltage controller could be fed forward with the circulating current $i_{circ,0}$ for improving the controllers response.

4.1.3. Droop Controlled Terminals

The droop controlled terminals are controlled in the PQ similarly to the slave terminals. The main difference is that the active power reference value is modulated according to the

measured DC voltage at the terminal as given by (15). The concept is analogous to the power sharing between synchronous generators with a frequency droop control operating in a power system.

The block diagram for the output current control of a droop controlled terminal is shown in Figure 8. In this figure, P^* is the active power reference provided by the system operator, $\overline{P}$ is the modulated active power reference and K_d is the DC voltage droop coefficient.

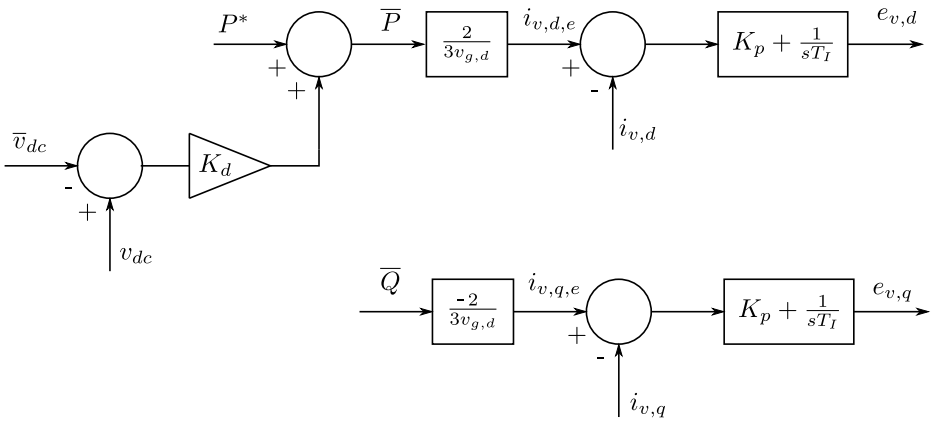

Figure 8. Output current controller of a droop controlled terminal.

The droop control terminals simulated in this work are also equipped with the internal dynamics controller shown in Figure 6 that is detailed in Section 4.1.1. It is worth mentioning that without a secondary control level, the droop controlled MT-HVDC network is subjected to a steady state error in the DC voltage level following a disturbance. The same is observed in the frequency of AC power systems where the frequency droop is used as the power sharing method.

4.2. Simulation Results

The system shown in Figure 4 is implemented in Matlab's Simscape Electrical. The parameters of the simulation are given in Table 2.

Table 2. Parameters of the simulated MT-HVDC network.

Parameters of Terminal 1					
Rated Power	900 MVA	AC Voltage	230 kV	AC frequency	50 Hz
Arm Resistance	1 Ohm	Arm Inductance	40 mH	DC Voltage	400 kV
Parameters of Terminals 2 and 3					
Rated Power	450 MVA	AC Voltage	132 kV	AC frequency	50 Hz
Arm Resistance	0.5 Ohm	Arm Inductance	40 mH	DC Voltage	400 kV

The simulations were performed according to two scenarios to illustrate the master/slave (denoted in the figure legends as *MS*) and the droop (denoted in the figure legends as *droop*) control methods. In the first scenario, the role of the master converter is attributed to Terminal 1, whilst Terminals 2 and 3 are the slave terminals. In the second scenario, Terminal 1 and Terminal 3 are equipped with droop control whilst Terminal 2 is controlled in *PQ* mode.

To simulate a disturbance in the wind speed, Terminal 2 follows a sequence of step changes in the reference value P^* as seen in Table 3. The load of the O&G platform conglomerate represented by the load in Figure 4 is assumed as constant and the variations seen in Table 3 are caused by the wind speed change. When the active power is positive, the load is bigger than the wind production, resulting in power delivery to Terminal 2.

When the active power reference is negative, it means that the wind power production is bigger than the load, resulting in a reversal of the active power flow in Terminal 2. Terminals 1 and 3 are assumed to keep constant power injections during the 5 s simulations. This means that no change in the power delivered to the continent are registered and that the wind remains at a constant speed in Terminal 3.

Table 3. Active power references for the slave terminals.

Time (s)	**0**	**1**	**2**	**3**	**4**
Terminal 2 Power (MW)	200	150	−100	200	300

Table 3, (14) is used to calculate the references for the inner current loop as shown in Figure 5. The output current response of Terminal 2 is shown in Figure 9. The controller in the dq frame is able to track the reference $i_{v,d,e}$ when it changes accordingly to the values calculated from Table 2. Furthermore, Figure 9 show the output current of Terminal 2 when the MT-HVDC network is droop controlled. Since the control strategy implemented in Terminal 2 does not change between the scenarios considered, the output currents from both scenarios present the same behavior when following the reference values obtained from Table 3.

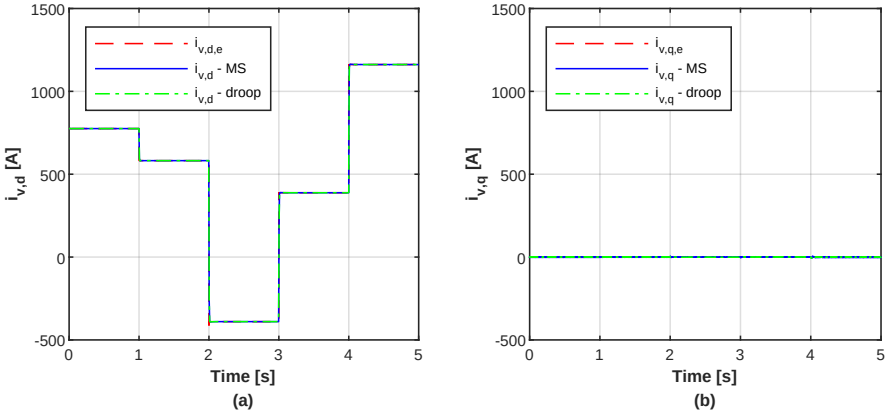

Figure 9. Output current response from terminal 2: (**a**) $i_{v,d}$; (**b**) $i_{v,q}$.

As hinted by the MMC model, changes in the output current and in the DC voltage are seen as disturbances by the internal dynamics of the converter. When the output current suddenly changes as seen in Figure 9, it causes a disturbance in the energy difference and in the converter energy. The energy dynamics responses are shown in Figure 10.

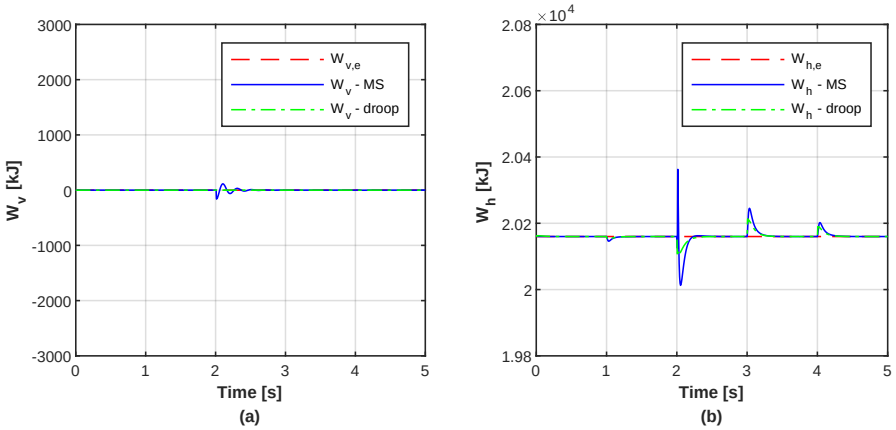

Figure 10. Energy dynamics response from terminal 2: (**a**) energy difference W_v; (**b**) total energy W_h.

From Figure 10, it can be noted that when the MT-HVDC network is droop controlled, the internal energy dynamics present a smoother response. The internal energy W_h is subjected to a smaller excursion from its reference value. The control of the energy dynamics is achieved by the cascaded control shown in Figure 6, manipulating the references for the circulating currents $i_{circ,d,e}$ and $i_{circ,0,e}$. The circulating current responses are shown in Figure 11.

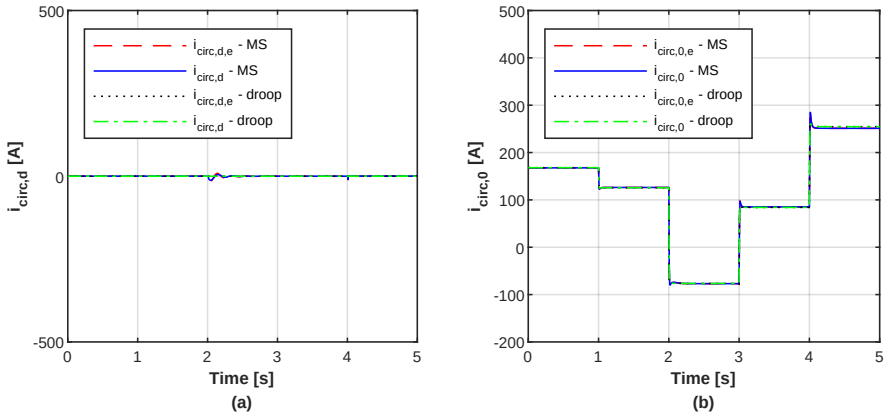

Figure 11. Circulating current response from terminal 2: (**a**) $i_{circ,d}$; (**b**) $i_{circ,0}$.

The 0-component of the circulating current presents a smaller overshoot when the MT-HVDC network is droop controlled. This is better seen in the step transition occurring at $t = 4$ s.

The sudden active power step changes in Terminal 2 result in a sequence of disturbances in the DC voltage of the MT-HVDC network. In Master/Slave operation, by demanding/injecting more power from/into the MT-HVDC network, the master terminal (Terminal 1) must act to keep the DC voltage at the desirable levels. In the droop controlled MT-HVDC network, the active power reference of Terminals 1 and 3, that are equipped with droop control, are modulated to perform power sharing among them.

By adopting the strategies presented in Figures 7 and 8, the DC voltage response in both scenarios is shown in Figure 12.

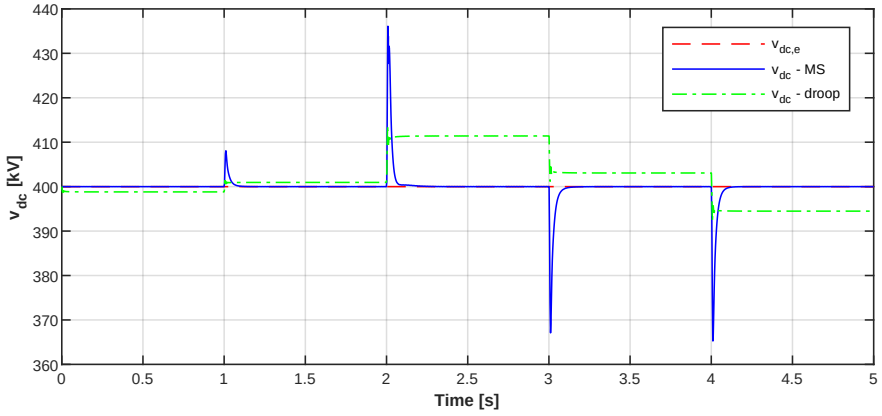

Figure 12. DC voltage measured at the master terminal.

When the Master/Slave concept is applied to the MT-HVDC network, the controller is able to regulate the DC voltage to its rated value of 400 kV. The worst disturbance is an overshoot of 9% over the rated DC voltage following the disturbance at $t = 2$ s and of 8.5% under the rated DC voltage for $t = 4$ s, respecting the $\pm 10\%$ thresholds suggested by [52]. A smoother response is obtained when the droop control is employed at the MT-HVDC network. Following the disturbance at $t = 2$ s, the worst deviation of the DC voltage is

2.85% over its rated value and the worst deviation under the rated value is of 1.37% for the disturbance considered, respecting the ±5% thresholds suggested by [53]. However, it can be seen that with the droop controller there is a steady-state error in the tracking of the DC voltage. If critical to the applications involved, the steady-state error could be eliminated by employing a secondary controller similar to the secondary frequency response in AC power systems.

In the Master/Slave controller grid, the DC voltage is regulated by acting on the reference value of the output current component $i_{v,d,e}$. When the droop control strategy is used, the DC voltage is regulated by modulating the active power references of the droop controlled terminals. The output current response for Terminal 1 in both cases is shown in Figure 13.

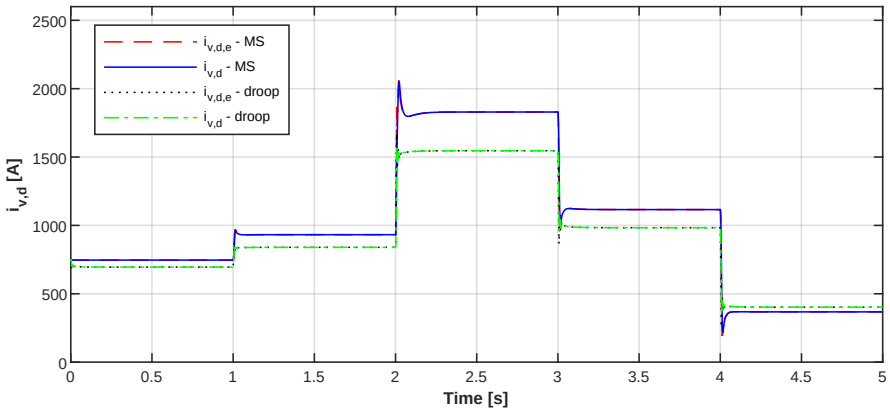

Figure 13. Output current component $i_{v,d}$ response of the master terminal.

The cascaded control structure of the Master/Slave concept is able to regulate the DC voltage of the MT-HVDC network. However, the PI controller is designed around a linearized model of the system. In the case of the disturbances caused by the power flow reversion, it is evident that the controller could present a better performance. Therefore, more complex techniques for the design of the Master/Slave operation such as the model predictive control and nonlinear control could be employed to improve the performance. However, by employing the droop control concept, the control effort on Terminal 1 is reduced since it is able to share the DC voltage control burden with Terminal 3. Therefore, this strategy is able to better cope with the nonlinearities of the system.

Since the energy dynamics are coupled with the both output and the circulating currents, the disturbances generated in the DC voltage will impact W_v and W_h. The energy dynamic response is shown in Figure 14 for both scenarios analyzed. Terminal 1 presented a smoother energy response when the MT-HVDC network is droop controlled.

The energy dynamics are controlled by the cascaded structure of Figure 6. Hence, it is noteworthy to analyze the response of the circulating currents shown in Figure 15.

In the Master/Slave scenario, it can be seen that the 0-component of the circulating current is regulated to the same value throughout the simulation due to the absence of power sharing. In the droop controlled scenario, the 0-component of the circulating current follows a similar profile than the output current shown in Figure 13, following the active power reference modulations resulting of theDC voltage deviation from its rated value.

Finally, we analyze the third terminal of the MT-HVDC network. Terminal 3 integrates an offshore wind farm into the MT-HVDC network. Its output current response in both scenarios is shown in Figure 16.

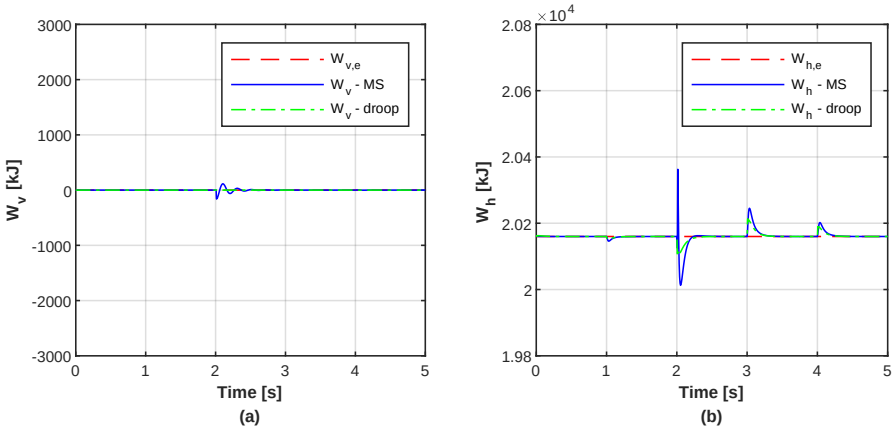

Figure 14. Energy dynamics response from the master terminal: (**a**) energy difference W_v; (**b**) total energy W_h.

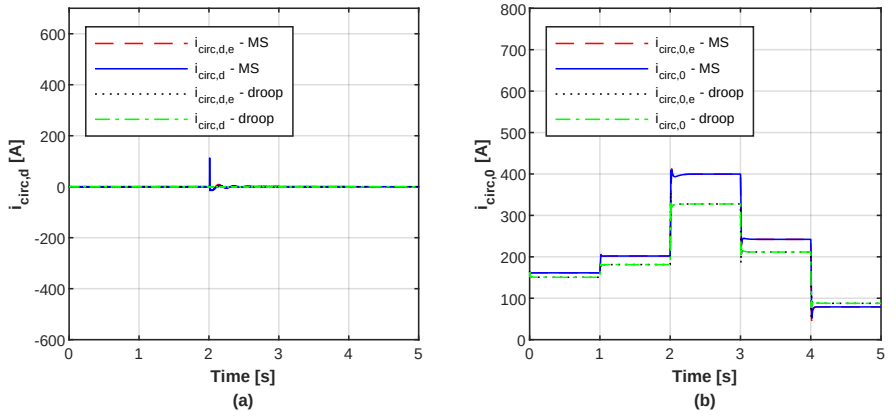

Figure 15. Circulating current response from the master terminal: (**a**) $i_{circ,d}$; (**b**) $i_{circ,0}$.

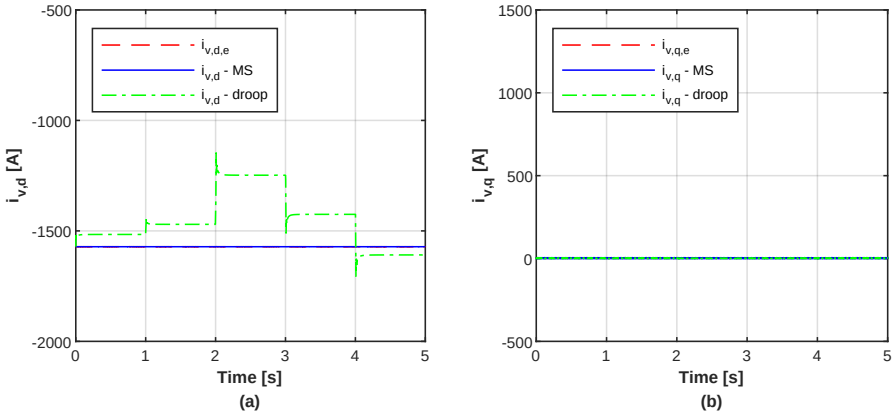

Figure 16. Output current response from terminal 3: (**a**) $i_{v,d}$; (**b**) $i_{v,q}$.

It is possible to note the effect of the droop control when comparing both responses. In Master/Slave control, there is no power sharing between the terminals of the network. Therefore, the active power output of Terminal 3 does not change throughout the simulation. When power sharing is enabled by the droop control, the active power reference of Terminal 3 is modulated to help Terminal 1 to control the DC voltage.

For Terminal 3 in Slave mode, the changes in the DC voltage following the active power step changes in Terminal 2 are the main disturbances. For the droop controlled scenario, the changes in the output current of Terminal 3 are additional disturbances given the droop control active power reference modulation. The energy dynamics response and

the manipulation of the circulating currents following the control structures shown in this section can be seen in Figures 17 and 18, respectively.

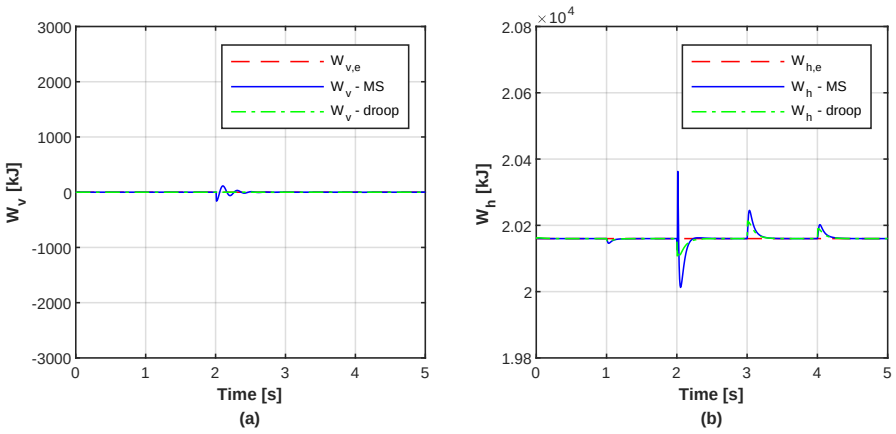

Figure 17. Energy dynamics response from terminal 3: (**a**) energy difference W_v; (**b**) total energy W_h.

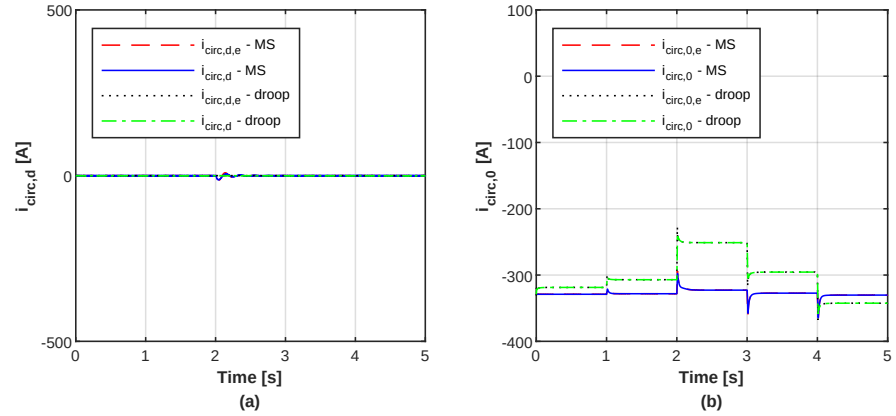

Figure 18. Circulating current response from terminal 3: (**a**) $i_{circ,d}$; (**b**) $i_{circ,0}$.

The cascaded control structure based on PI controllers developed in the synchronous reference frame shown in this section for both Master/Slave and droop control operation is able to meet the control objectives of each terminal. The power sharing established by the droop control accepts a deviation from the rated value of the DC voltage bu presents a smoother response than the Master/Slave control mode for the three-terminal network simulated in this work. The choice of a control system however will depend on the operation restrictions of each grid, whether the DC voltage levels should be sustained as close as possible to the rated value or if small steady state error are tolerated.

5. Conclusions

This paper presents a review on the main challenges concerning MT-HVDC networks for wind power integration. The characteristics of existing MT-HVDC networks are presented followed by a discussion of the rising challenges on control, operation, stability and protection. Then, the paper focused on the review of the main control alternatives for the DC voltage of an MT-HVDC network. The modeling and possible control strategies for the MMC were also discussed as a part of the review. To illustrate the technical discussions, a simulation of a three-terminal MT-HVDC network for the integration of wind power and other offshore resources is implemented on Matlab's Simscape Electrical following a PI-based control scheme in the $dq0$ frame, considering both the output current and the internal converter dynamics. The simulation results show the challenges on controlling a highly interconnected system as the MT-HVDC networks based on MMC converters. As MT-HVDC networks evolve and more projects are being currently considered, the problems

for the integration of growing shares of converter-based resources shall be further investigated. New models for stability analysis need to be developed to increase the knowledge of power system operators regarding the operation of DC grids.

Author Contributions: Conceptualization L.F.N.L., G.D. and A.J.S.F.; Writing—original draft preparation: L.F.N.L. and G.D.; writing—review and editing: L.F.N.L., G.D., M.N., M.D.-H., S.G., A.J.S.F. and L.M.; figure editing and validation: L.F.N.L., G.D., M.N., M.D.-H., S.G., A.J.S.F. and L.M.; simulations A.L., L.F.N.L. and G.D.; results discussion and validation L.F.N.L., G.D., M.N., M.D.-H., S.G., A.J.S.F. and L.M.; test system definition: L.F.N.L., G.D. and A.L. All authors have read and agreed to the published version of the manuscript.

Funding: This research was partly by the Laboratoire International Associé SEnSIN-CT between University Gustave Eiffel and Politecnico di Milano, and partly funded by the Coordenação de Aperfeiçoamento de Pessoal de Nível Superior – Brasil CAPES (Project 001), the National Council for Scientific and Technological Development (CNPq) grant number Process 405757/2018-2, and 407867/2022-8 and by the São Paulo Research Foundation Fapesp grant#2021/10421-0 and grant# 2022/00323-3.

Conflicts of Interest: The authors declare no conflict of interest. The funders had no role in the design of the study; in the collection, analyses, or interpretation of data; in the writing of the manuscript; or in the decision to publish the results.

Abbreviations

AC	Alternating current
CSC	Current Source Converter
DC	Direct Current
DFIG	Doubly Fed Induction Generator
HVDC	High Voltage Direct Current
LCC	Line Comutated Converter
MMC	Modular Multilevel Converter
MT-HVDC	Multi-Terminal High Voltage Direct Current
O&G	Oil and Gas
PI	Proportional-Integral Controller
PWM	Pulse Width Modulation
RES	Renewable Energy Sources
SG	Synchronous generator
VSC	Voltage source converter

References

1. Milano, F.; Dörfler, F.; Hug, G.; Hill, D.J.; Verbič, G. Foundations and challenges of low-inertia systems. In Proceedings of the 2018 Power Systems Computation Conference (PSCC), Dublin, Ireland, 11–15 June 2018; pp. 1–25.
2. Hatziargyriou, N.; Milanovic, J.; Rahmann, C.; Ajjarapu, V.; Canizares, C.; Erlich, I.; Hill, D.; Hiskens, I.; Kamwa, I.; Pal, B.; et al. Definition and classification of power system stability revisited & extended. *IEEE Trans. Power Syst.* **2020**, *36*, 3271–3281.
3. Lunardi, A.; Normandia Lourenço, L.F.; Munkhchuluun, E.; Meegahapola, L.; Sguarezi Filho, A.J. Grid-Connected Power Converters: An Overview of Control Strategies for Renewable Energy. *Energies* **2022**, *15*, 4151. [CrossRef]
4. Babatunde, O.M.; Munda, J.L.; Hamam, Y. Power system flexibility: A review. *Energy Rep.* **2020**, *6*, 101–106. [CrossRef]
5. Das, P.; Mathuria, P.; Bhakar, R.; Mathur, J.; Kanudia, A.; Singh, A. Flexibility requirement for large-scale renewable energy integration in Indian power system: Technology, policy and modeling options. *Energy Strategy Rev.* **2020**, *29*, 100482. [CrossRef]
6. Matevosyan, J.; Du, P. Inertia: Basic concept and impact on ERCOT grid. In Proceedings of the 15th International Workshop Large-Scale Integration of Wind Power into Power Systems, Vienna, Austria, 15–17 November 2016.
7. International Energy Agency (IEA). *Status of the Power System Transformation: Power System Flexibility*; International Energy Agency: Paris, France, 2019.
8. Gonzalez-Torres, J.C.; Damm, G.; Costan, V.; Benchaib, A.; Lamnabhi-Lagarrigue, F. A novel distributed supplementary control of Multi-Terminal VSC-HVDC grids for rotor angle stability enhancement of AC/DC systems. *IEEE Trans. Power Syst.* **2020**, *36*, 623–634. [CrossRef]
9. Van Hertem, D.; Gomis-Bellmunt, O.; Liang, J. *HVDC Grids: For Offshore and Supergrid of the Future*; John Wiley & Sons: Hoboken, NJ, USA, 2016.

10. Jovcic, D.; Ahmed, K. *High Voltage Direct Current Transmission: Converters, Systems and DC Grids*; John Wiley & Sons: Hoboken, NJ, USA, 2015.
11. Bahrman, M.P.; Johnson, B.K. The ABCs of HVDC transmission technologies. *IEEE Power Energy Mag.* **2007**, *5*, 32–44. [CrossRef]
12. Beerten, J.; Belmans, R. Modeling and control of multi-terminal VSC HVDC systems. *Energy Procedia* **2012**, *24*, 123–130. [CrossRef]
13. Gomis-Bellmunt, O.; Sánchez-Sánchez, E.; Arévalo-Soler, J.; Prieto-Araujo, E. Principles of operation of grids of DC and AC subgrids interconnected by power converters. *IEEE Trans. Power Deliv.* **2020**, *36*, 1107–1117. [CrossRef]
14. Bergna, G.; Garcés, A.; Berne, E.; Egrot, P.; Arzandé, A.; Vannier, J.C.; Molinas, M. A generalized power control approach in ABC frame for modular multilevel converter HVDC links based on mathematical optimization. *IEEE Trans. Power Deliv.* **2013**, *29*, 386–394. [CrossRef]
15. Carrizosa, M.J.; Stankovic, N.; Vannier, J.C.; Shklyarskiy, Y.E.; Bardanov, A.I. Multi-terminal dc grid overall control with modular multilevel converters. *Записки Горного института* **2020**, *243*, 357–370.
16. Sánchez-Sánchez, E.; Prieto-Araujo, E.; Junyent-Ferré, A.; Gomis-Bellmunt, O. Analysis of MMC energy-based control structures for VSC-HVDC links. *IEEE J. Emerg. Sel. Top. Power Electron.* **2018**, *6*, 1065–1076. [CrossRef]
17. Sánchez-Sánchez, E.; Prieto-Araujo, E.; Gomis-Bellmunt, O. The role of the internal energy in MMCs operating in grid-forming mode. *IEEE J. Emerg. Sel. Top. Power Electron.* **2019**, *8*, 949–962. [CrossRef]
18. Khan, A.; Seyedmahmoudian, M.; Raza, A.; Stojcevski, A. Analytical review on common and state-of-the-art FR strategies for VSC-MTDC integrated offshore wind power plants. *Renew. Sustain. Energy Rev.* **2021**, *148*, 111106. [CrossRef]
19. Normandia Lourenço, L.F.; Perez, F.; Iovine, A.; Damm, G.; Monaro, R.M.; Salles, M.B. Stability Analysis of Grid-Forming MMC-HVDC Transmission Connected to Legacy Power Systems. *Energies* **2021**, *14*, 8017. [CrossRef]
20. Abu-Elanien, A.E.; Abdel-Khalik, A.S.; Massoud, A.M. Multi-terminal HVDC system with offshore wind farms under anomalous conditions: Stability assessment. *IEEE Access* **2021**, *9*, 92661–92675. [CrossRef]
21. Bompard, E.; Fulli, G.; Ardelean, M.; Masera, M. It's a bird, it's a plane, it's a ... supergrid!: Evolution, opportunities, and critical issues for pan-European transmission. *IEEE Power Energy Mag.* **2014**, *12*, 40–50. [CrossRef]
22. Van Hertem, D.; Ghandhari, M. Multi-terminal VSC HVDC for the European supergrid: Obstacles. *Renew. Sustain. Energy Rev.* **2010**, *14*, 3156–3163. [CrossRef]
23. Myklebust, H.; Eriksson, K.; Westman, B.; Persson, G. Valhall power from shore after five years of operation. In Proceedings of the 2017 Petroleum and Chemical Industry Conference Europe (PCIC Europe), Calgary, AB, Canada, 18–20 September 2017; pp. 1–4.
24. Jones, P.; Stendius, L.; Sweden, A. The challenges of offshore power system construction. Troll A, electrical power delivered successfully to an oil and gas platform in the north sea. In Proceedings of the European Wind Energy Conference, Athens, Greece, 28 February–2 March 2006; pp. 75–78.
25. Normandia Lourenço, L.F.; Pereira, D.F.; Monaro, R.M.; Salles, M.B.; Rosa, R.M. Assessment of an Isolated Offshore Power Grid Based on the Power Hub Concept for Pre-Salt Oil and Gas Production. *IEEE Access* **2022**, *10*, 87671–87680. [CrossRef]
26. Bathurst, G.; Bordignan, P. Delivery of the Nan'ao multi-terminal VSC-HVDC system. In Proceedings of the 11th IET International Conference on AC and DC Power Transmission, Birmingham, UK, 10–12 February 2015; pp. 1–6.
27. Tang, G.; He, Z.; Pang, H.; Huang, X.; Zhang, X. Basic topology and key devices of the five-terminal DC grid. *CSEE J. Power Energy Syst.* **2015**, *1*, 22–35. [CrossRef]
28. Sun, J.; Li, M.; Zhang, Z.; Xu, T.; He, J.; Wang, H.; Li, G. Renewable energy transmission by HVDC across the continent: System challenges and opportunities. *CSEE J. Power Energy Syst.* **2017**, *3*, 353–364. [CrossRef]
29. The World's First DC-Grid with HVDC Light Technology. Available online: https://www.hitachienergy.com/br/pt/about-us/case-studies/zhangbei (accessed on 10 October 2022)
30. Zheng, Z.; Wang, Y.; Zhang, D.; Song, R.; Li, C.; Zhang, T. Reliability Evaluation Model of Zhangbei Multi-Terminal HVDC Transmission System. In Proceedings of the 2019 IEEE International Conference on Energy Internet (ICEI), Nanjing, China, 27–31 May 2019; pp. 279–284.
31. Goodrich, J. The Birthplace of the AC Grid. *IEEE Spectr.* **2021**. Available online: https://spectrum.ieee.org/the-birthplace-of-the-ac-grid (accessed on 15 November 2022).
32. Cunningham, J.J. 89 Liberty Street: The Birthplace of Commercial Polyphase Power [History]. *IEEE Power Energy Mag.* **2018**, *16*, 88–101. [CrossRef]
33. Gonzalez-Torres, J.C.; Damm, G.; Costan, V.; Benchaib, A.; Lamnabhi-Lagarrigue, F. Transient stability of power systems with embedded VSC-HVDC links: Stability margins analysis and control. *IET Gener. Transm. Distrib.* **2020**, *14*, 3377–3388. [CrossRef]
34. Gonzalez-Torres, J.C.; Costan, V.; Damm, G.; Benchaib, A.; Bertinato, A.; Poullain, S.; Luscan, B.; Lamnabhi-Lagarrigue, F. HVDC protection criteria for transient stability of AC systems with embedded HVDC links. *J. Eng.* **2018**, *2018*, 956–960. [CrossRef]
35. Taranto, G.N.; Pontes, C.E.; Campello, T.M.; Almeida, V.A.; Graham, J.; Esmeraldo, P.C.; Schicong, M. Power flow control for an embedded HVDC link to integrate renewable energy in Brazil. *Electr. Power Syst. Res.* **2022**, *211*, 108504. [CrossRef]
36. Shah, R.; Sanchez, J.C.; Preece, R.; Barnes, M. Stability and control of mixed AC–DC systems with VSC-HVDC: A review. *IET Gener. Transm. Distrib.* **2018**, *12*, 2207–2219. [CrossRef]
37. Li, H.; Shair, J.; Zhang, J.; Xie, X. Investigation of Subsynchronous Oscillation in a DFIG-based Wind Power Plant Connected to MTDC Grid. *IEEE Trans. Power Syst.* **2022**. [CrossRef]

38. Matevosyan, J.; Badrzadeh, B.; Prevost, T.; Quitmann, E.; Ramasubramanian, D.; Urdal, H.; Achilles, S.; MacDowell, J.; Huang, S.H.; Vital, V.; et al. Grid-forming inverters: Are they the key for high renewable penetration? *IEEE Power Energy Mag.* **2019**, *17*, 89–98. [CrossRef]
39. Khan, S.A.; Wang, M.; Su, W.; Liu, G.; Chaturvedi, S. Grid-Forming Converters for Stability Issues in Future Power Grids. *Energies* **2022**, *15*, 4937. [CrossRef]
40. Rosso, R.; Wang, X.; Liserre, M.; Lu, X.; Engelken, S. Grid-forming converters: An overview of control approaches and future trends. In Proceedings of the 2020 IEEE Energy Conversion Congress and Exposition (ECCE), Detroit, MI, USA, 11–15 October 2020; pp. 4292–4299.
41. Rokrok, E.; Qoria, T.; Bruyere, A.; Francois, B.; Zhang, H.; Belhaouane, M.; Guillaud, X. Impact of grid-forming control on the internal energy of a modular multilevel converter. In Proceedings of the 2020 22nd European Conference on Power Electronics and Applications (EPE'20 ECCE Europe), Virtual, 7–11 September 2020; pp. 1–10.
42. Arévalo-Soler, J.; Sánchez-Sánchez, E.; Prieto-Araujo, E.; Gomis-Bellmunt, O. Impact analysis of energy-based control structures for grid-forming and grid-following MMC on power system dynamics based on eigenproperties indices. *Int. J. Electr. Power Energy Syst.* **2022**, *143*, 108369. [CrossRef]
43. Groß, D.; Sanchez-Sanchez, E.; Prieto-Araujo, E.; Gomis-Bellmunt, O. Dual-port grid-forming control of MMCs and its applications to grids of grids. *IEEE Trans. Power Deliv.* **2022**, *37*, 4721–4735. [CrossRef]
44. Rokrok, E.; Qoria, T.; Bruyere, A.; Francois, B.; Guillaud, X. Classification and dynamic assessment of droop-based grid-forming control schemes: Application in HVDC systems. *Electr. Power Syst. Res.* **2020**, *189*, 106765. [CrossRef]
45. Du, W.; Fu, Q.; Wang, H. Damping torque analysis of DC voltage stability of an MTDC network for the wind power delivery. *IEEE Trans. Power Deliv.* **2019**, *35*, 324–338. [CrossRef]
46. Fu, Q.; Du, W.; Wang, H.; Ren, B.; Xiao, X. Small-signal stability analysis of a VSC-MTDC system for investigating DC voltage oscillation. *IEEE Trans. Power Syst.* **2021**, *36*, 5081–5091. [CrossRef]
47. Fu, Q.; Du, W.; Wang, H.; Zheng, Z.; Xiao, X. Impact of the Differences in VSC Average Model Parameters on the DC Voltage Critical Stability of an MTDC Power System. *IEEE Trans. Power Syst.* **2022**. [CrossRef]
48. Huo, Q.; Xiong, J.; Zhang, N.; Guo, X.; Wu, L.; Wei, T. Review of DC circuit breaker application. *Electr. Power Syst. Res.* **2022**, *209*, 107946. [CrossRef]
49. Corzine, K.A.; Ashton, R.W. A new Z-source DC circuit breaker. *IEEE Trans. Power Electron.* **2011**, *27*, 2796–2804. [CrossRef]
50. Li, C.; Liang, J.; Wang, S. Interlink hybrid DC circuit breaker. *IEEE Trans. Ind. Electron.* **2018**, *65*, 8677–8686. [CrossRef]
51. Wang, W.; Barnes, M.; Marjanovic, O.; Cwikowski, O. Impact of DC breaker systems on multiterminal VSC-HVDC stability. *IEEE Trans. Power Deliv.* **2015**, *31*, 769–779. [CrossRef]
52. Kirakosyan, A.; Ameli, A.; El-Fouly, T.H.; El Moursi, M.S.; Salama, M.; El-Saadany, E.F. A Novel Control Technique for Enhancing the Operation of MTDC Grids. *IEEE Trans. Power Syst.* **2022**. [CrossRef]
53. Rouzbehi, K.; Candela, J.I.; Gharehpetian, G.B.; Harnefors, L.; Luna, A.; Rodriguez, P. Multiterminal DC grids: Operating analogies to AC power systems. *Renew. Sustain. Energy Rev.* **2017**, *70*, 886–895. [CrossRef]
54. Beerten, J.; Cole, S.; Belmans, R. Modeling of multi-terminal VSC HVDC systems with distributed DC voltage control. *IEEE Trans. Power Syst.* **2013**, *29*, 34–42. [CrossRef]
55. Chen, Y.; Carrizosa, M.J.; Damm, G.; Lamnabhi-Lagarrigue, F.; Li, M.; Li, Y. Control-induced time-scale separation for multiterminal high-voltage direct current systems using droop control. *IEEE Trans. Control. Syst. Technol.* **2019**, *28*, 967–983. [CrossRef]
56. Xiao, L.; Xu, Z.; An, T.; Bian, Z. Improved analytical model for the study of steady state performance of droop-controlled VSC-MTDC systems. *IEEE Trans. Power Syst.* **2016**, *32*, 2083–2093. [CrossRef]
57. Li, D.; Wu, Z.; Zhao, B.; Zhang, L. An improved droop control for balancing state of charge of battery energy storage systems in AC microgrid. *IEEE Access* **2020**, *8*, 71917–71929. [CrossRef]
58. Song, S.; McCann, R.A.; Jang, G. Cost-based adaptive droop control strategy for VSC-MTDC system. *IEEE Trans. Power Syst.* **2020**, *36*, 659–669. [CrossRef]
59. Pinto, R.T.; Bauer, P.; Rodrigues, S.F.; Wiggelinkhuizen, E.J.; Pierik, J.; Ferreira, B. A novel distributed direct-voltage control strategy for grid integration of offshore wind energy systems through MTDC network. *IEEE Trans. Ind. Electron.* **2012**, *60*, 2429–2441. [CrossRef]
60. Chaudhuri, N.R.; Majumder, R.; Chaudhuri, B. System frequency support through multi-terminal DC (MTDC) grids. *IEEE Trans. Power Syst.* **2012**, *28*, 347–356. [CrossRef]
61. Wang, W.; Li, Y.; Cao, Y.; Häger, U.; Rehtanz, C. Adaptive droop control of VSC-MTDC system for frequency support and power sharing. *IEEE Trans. Power Syst.* **2017**, *33*, 1264–1274. [CrossRef]
62. Xiong, Y.; Yao, W.; Shi, Z.; Fang, J.; Ai, X.; Wen, J.; Cheng, S.j. Adaptive Dual Droop Control of MTDC Integrated Offshore Wind Farms for Fast Frequency Support. *IEEE Trans. Power Syst.* **2022**. [CrossRef]
63. Xiong, Y.; Yao, W.; Yao, Y.; Fang, J.; Ai, X.; Wen, J.; Cheng, S. Distributed Cooperative Control of Offshore Wind Farms Integrated Via MTDC System for Fast Frequency Support. *IEEE Trans. Ind. Electron.* **2022**. [CrossRef]
64. Xiong, Y.; Yao, W.; Lin, S.; Ai, X.; Fang, J.; Wen, J.; Cheng, S. Improved Communication-Free Coordinated Control of VSC-MTDC Integrated Offshore Wind Farms for Onshore System Frequency Support. *IEEE Trans. Power Deliv.* **2022**. [CrossRef]

65. Kirakosyan, A.; El-Saadany, E.F.; El Moursi, M.S.; Salama, M.M. Selective frequency support approach for mtdc systems integrating wind generation. *IEEE Trans. Power Syst.* **2020**, *36*, 366–378. [CrossRef]
66. Antonopoulos, A.; Angquist, L.; Nee, H.P. On dynamics and voltage control of the modular multilevel converter. In Proceedings of the 2009 13th European Conference on Power Electronics and Applications, Barcelona, Spain, 8–10 September 2009; pp. 1–10.
67. Saad, H.; Guillaud, X.; Mahseredjian, J.; Dennetiere, S.; Nguefeu, S. MMC capacitor voltage decoupling and balancing controls. *IEEE Trans. Power Deliv.* **2014**, *30*, 704–712. [CrossRef]
68. Angquist, L.; Antonopoulos, A.; Siemaszko, D.; Ilves, K.; Vasiladiotis, M.; Nee, H.P. Open-loop control of modular multilevel converters using estimation of stored energy. *IEEE Trans. Ind. Appl.* **2011**, *47*, 2516–2524. [CrossRef]
69. Harnefors, L.; Antonopoulos, A.; Norrga, S.; Angquist, L.; Nee, H.P. Dynamic analysis of modular multilevel converters. *IEEE Trans. Ind. Electron.* **2012**, *60*, 2526–2537. [CrossRef]
70. Tu, Q.; Xu, Z.; Xu, L. Reduced switching-frequency modulation and circulating current suppression for modular multilevel converters. *IEEE Trans. Power Deliv.* **2011**, *26*, 2009–2017.
71. Harnefors, L.; Antonopoulos, A.; Ilves, K.; Nee, H.P. Global asymptotic stability of current-controlled modular multilevel converters. *IEEE Trans. Power Electron.* **2014**, *30*, 249–258. [CrossRef]
72. Antonopoulos, A.; Ängquist, L.; Harnefors, L.; Ilves, K.; Nee, H.P. Global asymptotic stability of modular multilevel converters. *IEEE Trans. Ind. Electron.* **2013**, *61*, 603–612. [CrossRef]
73. Prieto-Araujo, E.; Junyent-Ferré, A.; Collados-Rodríguez, C.; Clariana-Colet, G.; Gomis-Bellmunt, O. Control design of Modular Multilevel Converters in normal and AC fault conditions for HVDC grids. *Electr. Power Syst. Res.* **2017**, *152*, 424–437. [CrossRef]
74. Peralta, J.; Saad, H.; Dennetière, S.; Mahseredjian, J.; Nguefeu, S. Detailed and averaged models for a 401-level MMC–HVDC system. *IEEE Trans. Power Deliv.* **2012**, *27*, 1501–1508. [CrossRef]
75. Vatani, M.; Hovd, M.; Saeedifard, M. Control of the modular multilevel converter based on a discrete-time bilinear model using the sum of squares decomposition method. *IEEE Trans. Power Deliv.* **2015**, *30*, 2179–2188. [CrossRef]
76. Bergna, G.; Berne, E.; Egrot, P.; Lefranc, P.; Arzande, A.; Vannier, J.C.; Molinas, M. An energy-based controller for HVDC modular multilevel converter in decoupled double synchronous reference frame for voltage oscillation reduction. *IEEE Trans. Ind. Electron.* **2012**, *60*, 2360–2371. [CrossRef]
77. Bergna-Diaz, G.; Suul, J.A.; D'Arco, S. Energy-based state-space representation of modular multilevel converters with a constant equilibrium point in steady-state operation. *IEEE Trans. Power Electron.* **2017**, *33*, 4832–4851. [CrossRef]
78. de Oliveira, G.C.; Damm, G.; Monaro, R.M.; Normandia Lourenco, L.F.; Carrizosa, M.J.; Lamnabhi-Lagarrigue, F. Nonlinear control for modular multilevel converters with enhanced stability region and arbitrary closed loop dynamics. *Int. J. Electr. Power Energy Syst.* **2021**, *126*, 106590. [CrossRef]
79. Wu, M.; Li, Y.W.; Konstantinou, G. A comprehensive review of capacitor voltage balancing strategies for multilevel converters under selective harmonic elimination PWM. *IEEE Trans. Power Electron.* **2020**, *36*, 2748–2767. [CrossRef]
80. Dahidah, M.S.; Konstantinou, G.; Agelidis, V.G. A review of multilevel selective harmonic elimination PWM: Formulations, solving algorithms, implementation and applications. *IEEE Trans. Power Electron.* **2014**, *30*, 4091–4106. [CrossRef]
81. Antonio-Ferreira, A.; Collados-Rodriguez, C.; Gomis-Bellmunt, O. Modulation techniques applied to medium voltage modular multilevel converters for renewable energy integration: A review. *Electr. Power Syst. Res.* **2018**, *155*, 21–39. [CrossRef]
82. Samimi, S.; Gruson, F.; Delarue, P.; Colas, F.; Belhaouane, M.M.; Guillaud, X. MMC stored energy participation to the DC bus voltage control in an HVDC link. *IEEE Trans. Power Deliv.* **2016**, *31*, 1710–1718. [CrossRef]
83. Sanchez-Sanchez, E.; Gross, D.; Prieto-Araujo, E.; Dörfler, F.; Gomis-Bellmunt, O. Optimal multivariable MMC energy-based control for DC voltage regulation in HVDC applications. *IEEE Trans. Power Deliv.* **2019**, *35*, 999–1009. [CrossRef]
84. Samimi, S.; Gruson, F.; Guillaud, X.; Delarue, P. Control of DC bus voltage with a Modular Multilevel Converter. In Proceedings of the 2015 IEEE Eindhoven PowerTech, Eindhoven, The Netherlands, 29 June–2 July 2015; pp. 1–6.
85. Shinoda, K.; Benchaib, A.; Dai, J.; Guillaud, X. Virtual capacitor control: Mitigation of DC voltage fluctuations in MMC-based HVDC systems. *IEEE Trans. Power Deliv.* **2017**, *33*, 455–465. [CrossRef]
86. Yazdani, A.; Iravani, R. *Voltage-Sourced Converters in Power Systems: Modeling, Control, and Applications*; John Wiley & Sons: Hoboken, NJ, USA, 2010.
87. Bevrani, H.; François, B.; Ise, T. *Microgrid Dynamics and Control*; John Wiley & Sons Hoboken, NJ, USA, 2017.
88. Teodorescu, R.; Liserre, M.; Rodriguez, P. *Grid Converters for Photovoltaic and Wind Power Systems*; John Wiley & Sons Hoboken, NJ, USA, 2011; Volume 29,
89. Shinoda, K.; Benchaib, A.; Dai, J.; Guillaud, X. DC voltage control of MMC-based HVDC grid with Virtual Capacitor Control. In Proceedings of the 2017 19th European Conference on Power Electronics and Applications (EPE'17 ECCE Europe), Warsaw, Poland, 11–14 September 2017.